CHAPTER-2

LITERATURE REVEIW

2.1. Development of Al-Si-alloy based material for engine applications

As economic and environmental requirements are becoming more stringent day by day, it is imperative to reduce vehicle weight. With a view to this, hypoeutectic Al-Si alloys, Al 356.0 or Al 319.0 and hypereutectic alloy like Al 390.0 have been increasingly commercially employed for fabrication of engine block, liner, piston etc., primarily because of their high strength- to weight- ratio. The material replacement in engine block made of cast iron by aluminium could result in a slash in weight of 15–35 kg.[1-4]

Apart from light weight, in comparison with cast iron, aluminium alloys possess excellent thermal conductivity which accelerates cooling of engine. In spite of all these merits, major problem in hypoeutectic Al alloys which limits their application in engine components, is softening at service temperature. The 356-type aluminium alloys retains good combinations of tensile strength and ductility up to a temperature of about 200°C, but their strength reduces rapidly above 200°C. In contrast, the A319 alloys have comparatively higher yield and creep strength up to temperatures of approximately 250°C [3].

However, exposure at such temperatures for prolonged time causes softening. Another demerit of using hypoeutectic aluminum alloys is that, they do not possess the required wear characteristics for engine block material. Therefore, surface engineering capable to meet up these deficiencies in tribological characteristic are essential. Historically, the problem was solved by using ‘cast-in’ or ‘pressed-in’ cast iron sleeve or liner in the cylinder bores to fulfill the required surface tribological properties. Cast iron

liners are low-cost, durable, and easy to manufacture, which are the important criteria for mass scale productions [3,4].

Although, cast iron liners are a economic solution at the moment, they have the inherent disadvantages in weight, size, thermal conductivity, differential thermal expansion and recyclability compared to the potential alternative materials. The difference in co-efficient of thermal expansion of gray cast iron and the aluminum cylinder block material may lead to liner deformation and also local heat transfer problems. Consequently increased fuel consumption and increasing emissions are caused due to the deformation of the liner.

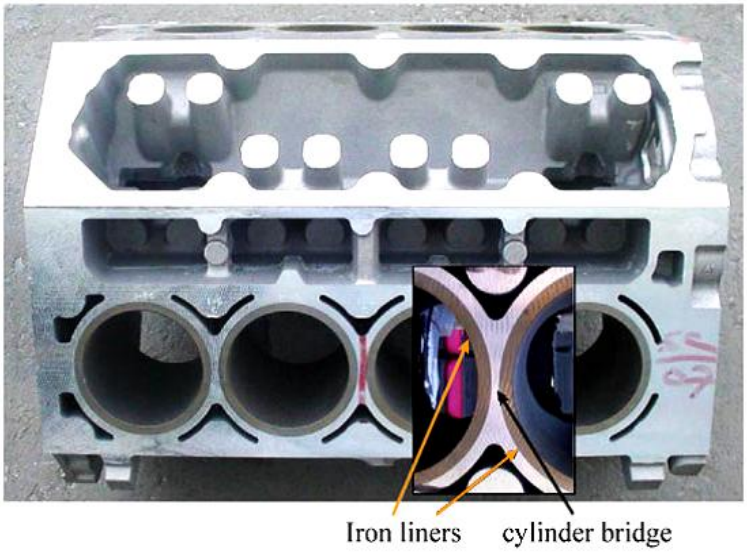

Fig.2.1. Engine block with cast-in liners [4].

An alternative approach prior to the development of cast iron liners was the use of hypereutectic Al-Si alloy like A390.0. Several favorable benefits could be obtained from hypereutectic alloys such as, improved thermal conductivity, provides required tribological surface characteristics, high cycle fatigue strength about 50% higher than that of hypoeutectic Al-Si alloys, low co-efficient of thermal expansion, high hardness and high ability to recycle.

However, certain demerits associated with hypereutectic Al–Si alloys are against their widespread application. The surface tribological properties of hypereutectic Al–Si alloys are strongly influenced by the even dispersion of hard Si particles. The casting process of the hypereutectic Al–Si alloys with homogeneous and uniform dispersion of Si particles is really difficult. Moreover, to improve the mechanical properties expensive additions like Ni is needed which adds to manufacturing cost. Another demerit is that hypereutectic Al-Si alloys are subjected to a honing process which is a chemical etching process to protrude primary silicon particles from the Al cylinder bore surface. This additional process step increases processing time and costs.

The second potent alternative for replacing the traditional aluminium cylinder block fitted with cast iron liner is by use of metal matrix composites (MMCs). MMCs can be employed in two ways- either the entire cylinder block can be made up of monolithic MMCs or only cylinder liner made of MMCs could be placed into a hypoeutectic Al–Si alloy cylinder block. An MMC is constituted with minimum two distinct phases, properly distributed to result in a unique combinations of properties which are not attainable by the individual components. It comprises of a matrix and reinforcements (fibrous or particulate phase), in which the reinforcements are surrounded by the matrix. The primary objective of addition of hard ceramic reinforcements is to increase hardness which will consequently increase the wear resistance. Most commonly used hard phase in Al-Si alloys are SiC and Al_2O_3. To impart a solid lubricating effect, soft secondary particles/fibres (e.g. graphite and MoS_2) are often added into the matrix to decrease the friction, consequently reduction of wear.

Several benefits can be obtained with MMC lined cylinder blocks which includes lower thermal deformation, more thermally conductive and lower bore-to-bore distance

compared to cast iron liners. Moreover, the processing of cylinder blocks lined with MMC are easier than hypereutectic Al–Si alloy cylinder blocks.

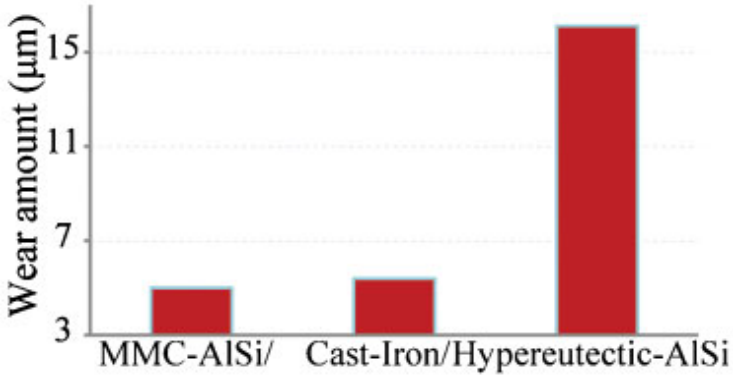

Fig.2.2. Wear amount of different cylinder bore material [5].

There are certain drawbacks in material characteristics which prevent total replacement of cast iron liners by metal matrix composites. An even distribution of reinforcing particles throughout the cylinder bore surface is essential otherwise it will cause engine failure. The piston ring tends to wear away the softer aluminum matrix lean in the reinforcement particles. Once the cylinder bore is worn out, compression is lost and engine failure will occur. The reinforcement distribution should be capable of impregnation of oil film during operation. A effective contact area between the piston ring material in absence of an oil film will result in premature wear and scuffing. After repeated contacts, the reinforcement material may be fragmented if there is too much point contact with the piston rings.

Other two alternatives to replace the cast iron liners for aluminum alloy cylinder blocks is either to provide coating on the cast aluminum block cylinder bores by thermal spraying of wear resistant, ceramic or composite material or to electroplate with high hardness, wear resistant materials. In the first case, the spraying of molten metal forms a hard facing to develop wear resistant surface whereas in the electroplating processes are

nickel ceramic composite (NCC) coatings, and plasma electrolytic oxidation (PEO) coatings. The most basic of the drawbacks of the thermal spray coatings is the weakness of the bond between the coated material and the aluminum. With improper coating, the coating is delaminated in-service, and exposing the soft aluminum block material. This will cause premature wearing and eventually the engine will lose compression resulting in engine failure. In case of electroplating, sulfur present in gasoline breaks the nickel based coating causing leak down and subsequently total engine failure.

A highly promising alternative is functionally graded in-situ Al- Mg_2Si composite liner in which the highly populated reinforcement in the inner surface are able to improve the inner surface wear properties. The primary Mg_2Si particles are segregated in the inner layer of castings by the centrifugal action with relatively smaller densities (ρ_{Mg2Si}= 1:99 g/cm^3) than that of Al melt (ρ_{Al} = 2.37 g/cm^3). As the volume% of Mg_2Si is gradually decreasing towards outer layer of the casting the ductility and toughness are not impaired.

2.2. Functionally Graded Materials (FGM)

Functionally graded materials (FGMs) are advanced engineering materials purposely designed with a spatial gradation in microstructure and/or composition which results in it tailored properties for a specific application or function. Interest in FGMs has recently enormously increased because of their ability to produce materials with tailored properties which are suitable candidates for numerous aerospace, bio-engineering and nuclear applications. The gradual volume fraction change in of the FGM components and inhomogenous structure generates continuous graded macroscopic properties, viz. hardness, wear resistance, corrosion resistance, thermal conductivity, specific heat and density [5-8].

2.2.1. Fabrication processes of bulk FGMs

The fabrication process of a FGM can generally be divided based on generation of the spatially inhomogeneous structure ("gradation") and subsequently the structure is transformed into a bulk material ("consolidation"). Gradation processes can again be sub-divided into constitutive, homogenizing and segregating processes. Constitutive processes involve a stepwise formation of the graded structure from initial precursor materials or powders. The sharp interface between precursor and the actual material is then converted into a gradient by material transport in homogenizing processes. Segregating processes convert macroscopically homogeneous material into a graded material by material transport with the help of an external field like gravitational or electric field. Homogenizing and segregating processes generate continuous gradients; however have limitations in regard to the types of gradients produced.

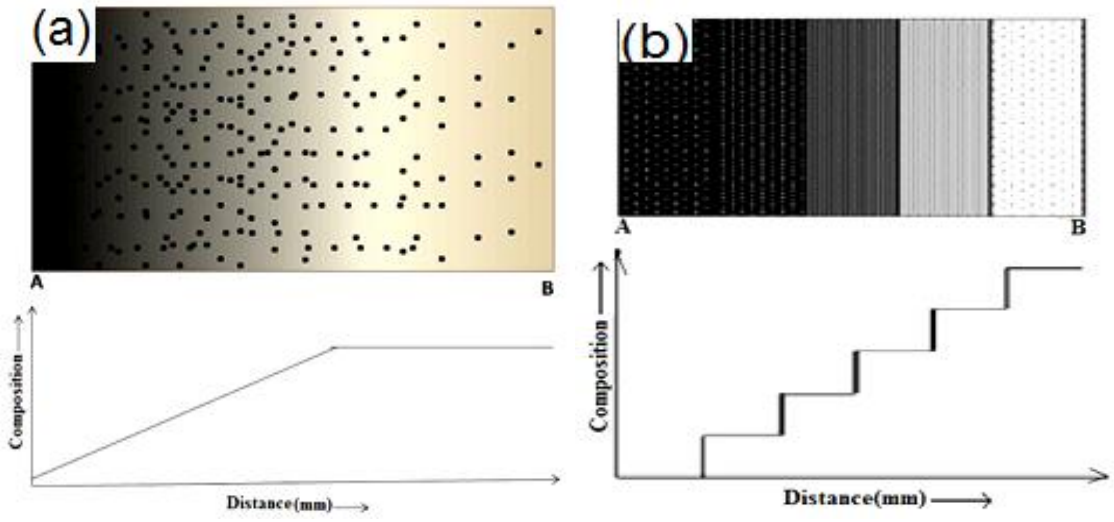

Fig.2.3. Types of Graded structure (a) continuous graded structure (b) stepwise graded structure.

2.2.1.1. Powder metallurgy

The powder metallurgy (PM) or ceramic technology route as fabrication process engineering parts comprise of powder production, processing of powder, shaping by compaction and sintering or pressure assisted hot consolidation. Powders of wide size ranges from nanometers to several hundred micrometers of different metals, alloys, compounds and ceramic materials are available or may be produced by standard methods. Powder mixtures with varied average particle size or composition are taken during deposition of the material before the forming or compaction operation. The method applied for powder deposition dictates whether variation in the green body will be smooth or in steps. Since the consolidation of the green parts during sintering or hot pressing requires high temperatures at which diffusion processes are rapid enough for densification, chemical reactions between particles of different compositions and the influence of particle size on the sintering behavior are considered for the final microstructure and dimensional control of the part. Beside these, thermodynamic factors during sintering may be utilized to create a gradient, example is during liquid-phase sintering.

Jin et al. [9] studied development of functionally graded Mullite/Mo by powder metallurgy technique. The selection was based on the similar coefficients of thermal expansion of the components. Mechanical properties and thermal behavior of FGM samples are found to follow the Voigt model and Reuss model, respectively. Surface crack initiation and propagation are correlated with dispersion of thermal stress during cooling. Thermal stresses developed from high cooling rate creates a distance from the coolest part and capable of arresting cracks due to a lower amount of residual stresses.

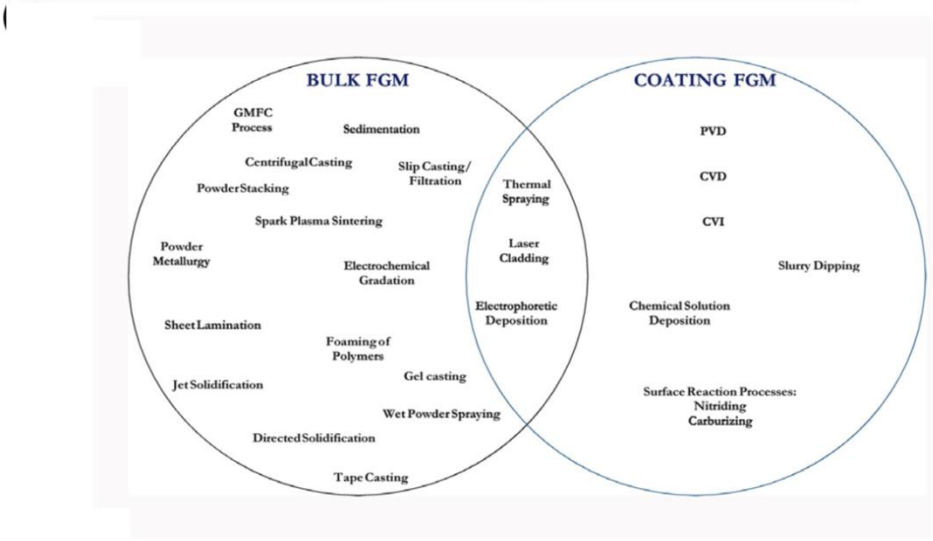

(a)

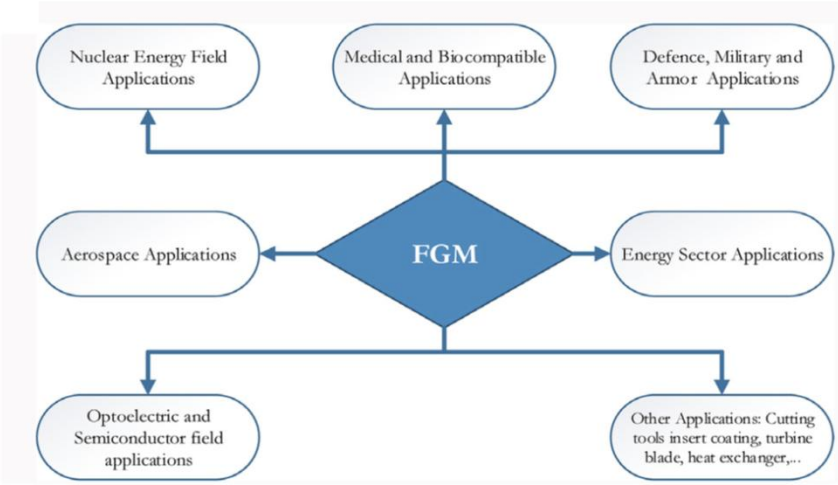

(B)

Fig. 2.4. (A) Various fabrication methods for bulk and coating type functionally graded materials. (B) Diverse application fields of FGMs [8].

An analysis of the effect of both adding SiC powders and the initial phase powder grain size on the mechanical and structural properties of function-ally graded Ti/TiB_2 has been conducted [10]. Ti/TiB_2 specimens which used SiC as a sintering aid had been

observed to have higher flexural strength and toughness compared to other FGMs. Formation of SiO2 during the fabrication of FGM changes the sintering mechanism and leads to the densification of powders through liquid phase sintering. It is confirmed that with increase in amount of SiC, theTiB2 layers density was increased.

Development of functionally graded Ti-TiB for ballistic application is reported [11] by hot pressing (liquid phase pressure sintering) or pressure assisted densification (PAD) method. The residual stress drawback in the fabrication could be avoided by the functionally graded TiB ballistic material. The volume fraction of TiB in the FGM strongly influences the co-efficient of thermal expansion, ballistic performance and mechanical property, particularly the Young's modulus. In another work by Übeyli et al.[12] the ballistic performance of a SiC–AA7075 FGM specimen was assessed; fabricated by powder metallurgy with various thicknesses using armour piercing projectile. Specimen thicknesses > 25 mm showed improved ballistic performance. Fracture analysis of specimens revealed a brittle fracture in FGMs with some fine cracks at macro level and some microcracks and deformed grains near to the zones of loading.

FGM of Al_2TiO_5/Al_2O_3 system has been reported [13] with varying volume contents of Al_2TiO_5 by powder metallurgy sintering. The thermal stresses generated in the production process have been simulated by finite element method. The optimum distribution of Al_2TiO_5/Al_2O_3 with respect to composition, FGMs has been developed with a minimum residual thermal stress. A reactive hot-pressing method is developed by Brinkman et al.[14] allowing material flow during the transient liquid stage. Al-TiB_2 composites with a high volume% of TiB_2 near the ingot surface and leaning towards centre.

Another sintering method often used for FGM production is spark plasma sintering (SPS). The merits and limitations of this method are reported [15]. The SPS method was employed for preparation of $Cu/Al_2O_3/Cu$[16], $Ni/Al_2O_3/Ni$[17], $TiB_2/AlN/Cu$[18,19] FGMs and AlN based composites[20]. Graded Cu/AlN/Cu composites have been manufactured by two step SPS method to produce electrodes for thermoelectric generators [21]. Initially porous graded AlN plate was prepared with AlN powder of different sizes then graded Cu/AlN/Cu samples have been made by impregnation of Cu into the pores of the external porous AlN layer.

2.2.1.2. Liquid phase processes

a) Centrifugal casting

In centrifugal casting process of metal based FGMs, the reinforcement phase is poured into a molten metal to make a uniform mixture. Through segregation of reinforcement particles and liquid by gravitational/centrifugal forces, a designed gradient in the chemical composition is created and maintained by controlling the solidification process [22]. Watanabe et al. [23] reported the fabrication of a controlled wall thickness metal tube by centrifugal casting technique. Molten metal with ceramic particulates was subjected to centrifugal force to produce a graded chemical composition in FGM [24].

Based on the difference between parent metal temperatures and processing temperature, two different categories of centrifugal casting methods exist(Fig.2.5). Centrifugal in-situ technique involves the processing at temperature higher than the parent alloy liquidus temperature and centrifugal forces can be used during the solidification step. If the processing temperature is below the parent alloy liquidus temperature the second phase remains solid in the molten metal and this is known as the centrifugal solid-particle

technique [25]. A mathematical approach of diffusion mechanism and bonding property of metal matrix composites (MMCs) has also been reported [26,27].

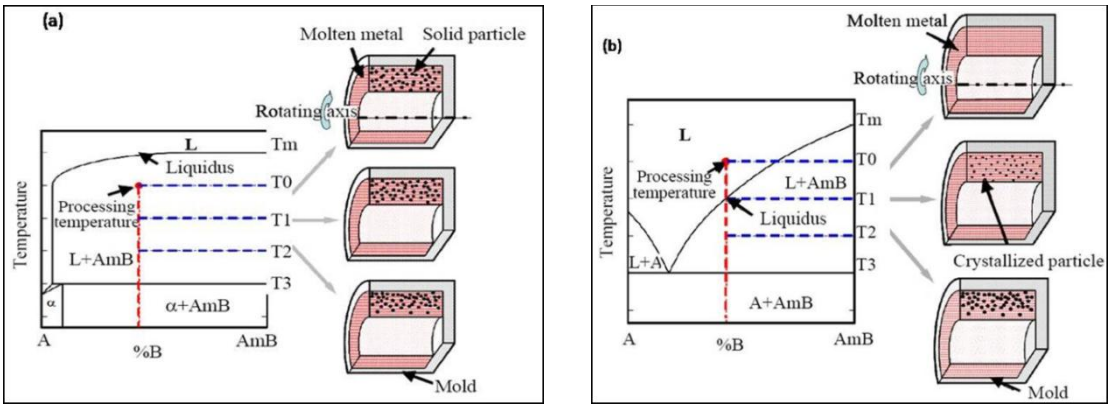

Fig.2.5. Schematic Illustration of Processing Temperature (a) Centrifugal Solid Particle and (b) In-situ Methods [25].

The technique is widely employed for different types of metal-intermetallic and metal-ceramic FGMs fabrication [28,29]. In spite of having mass production capability a precise control should be exercised for uniform distribution of second phase. The composition gradient in the FGMs is basically influenced by the heating/cooling control system and mould rotating speed. Inability of production through other process routes like forging (i.e. poor degree of deformability) and powder metallurgy (P/M)(i.e. limited formability of TiAl alloy) provokes use the centrifugal casting method. Fu et al. [30] examined influence of different key process parameters like pouring temperature, mould temperature and mold rotation speed on TiAl system. Fukui [31] studied the theoretical principles of production of FGMs by centrifugal casting method with plaster and corundum mixture of different volume fractions and processing time. A mathematical expression and model showing the changes in volume fraction and time have been proposed. A relation between the gradient of volume fraction of powders and centrifugal load was established.

The fabrication of aluminium-silicon carbide graded composite by centrifugal casting method has been reported by Rajan et al.[32] . Maximum SiC particulates of 45% in Al-A356 and 40% in Al2124-based MMCs, respectively were observed close to the outer circumference. Subsequent heat treatment provides formation of extra hard precipitate phase in the matrix and a considerable increase in hardness observed. A sharp transition in Al-A356 alloy was observed whereas in 2124 alloy transition was gradual due to differences in amounts of eutectic liquid in those systems (Al-A356 alloy contains more liquid eutectic compared to Al2124 alloy). Further the freezing range of 2124 alloy (637–490°C) is wider than that of 356 alloy (615–564°C) and the viscosity of alloys has a strong effect on the nature of transitions from the SiC enriched to the leaner zone (Fig.2.6). High specific strength, increased surface hardness and consequent wear resistance can be developed from Al-SiC FGMs produced through centrifugal casting route.

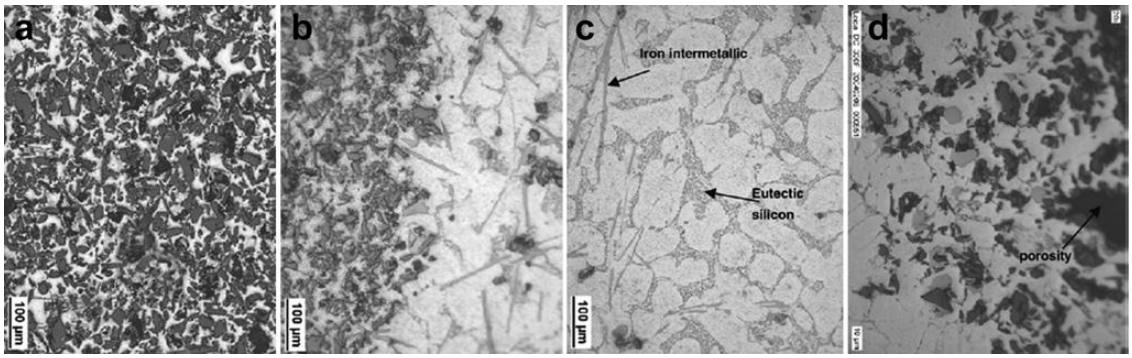

Fig.2.6. Centrifugally cast graded microstructure in different region of A356-SiC_P composite (a) 1.5 mm; (b) 5.5 mm; (c) 6.5 mm; (d) 15 mm. Distances are away from outer surface of the cylindrical casting[32].

In a similar work, Rodrı´ıguez-Castro et al. [33] investigated the effect of SiC particles on the mechanical behavior and microstructural features of functionally graded Al359/SiCp. With centrifugal casting method, SiC content and consequent elastic moduli were observed to be changed continuously. Up to 0.2-0.3 volume fraction of SiC, tensile

strength increases but further increase of SiC to 0.3- 0.4, causes UTS to decrease. However, elastic modulus and stiffness were increased with SiC volume fractions. The fracture showed under SEM, a ductile nature of failure. The mechanical properties of the FGM are influenced by the mechanism of void growth changing with SiC concentration, de-cohesion and particulate-fracture. The hard reinforcing particles are reported to repel matrix plastic deformation at the crack end. Watanebe et al. [34] investigated the manufacture a nickel-aluminide/steel clad pipe. The process involves placing Ni powders inside of a steel pipe and pouring liquid aluminum. A composite layer by exothermic heat of melting reaction was produced by the reaction between aluminum and Ni powder. This study assessed the effect of the spinning angle of the centrifugal castors. Coating area had an inverse related to the angle of the mould axis. The best homogeneity and uniformity of composite was observed in a horizontal centrifugal casting machine.

Sequeira et al.[35,36] have studied Al-Al3Zr and Al-Al3Ti FGMs developed by centrifugal solid –particle method using Al-5 wt% Zr and Al-5 wt% Ti commercial alloys, respectively. The operating temperatures were below the liquidus temperatures of the alloys where majority of the intermetallic platelets are solid in a liquid matrix. Because of the higher relative densities of Al_3Zr and Al_3Ti intermetallics these are segregated at the outer periphery of the tubes mostly orientated perpendicular to the centrifugal force (Fig.2.7). Remarkable increase in hardness up to three times has been obtained in intermetallic reinforcement rich regions. The formation of FGMs with Al-Al_2Cu have also been studied by centrifugal casting technique [37,38]. In-situ Al-Al2Cu FGMs have been produced with eutectic (Al-33 wt% Cu), hypoeutectic, and hypereutectic alloys. The microstructure of the FGMs has been explained based on the Al-Cu phase diagram.

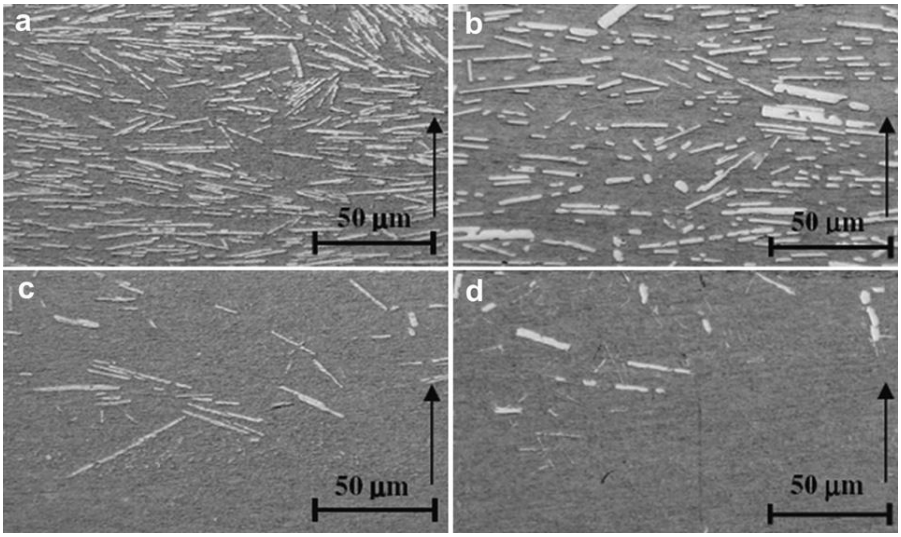

Fig.2.7. Optical micrographs of different regions of FGMs,: (a) and (b) are from Al-Al3Ti FGM in outer and inner regions, respectively; (c) and (d) are from Al-Al_3Zr FGM in outer and inner regions, respectively. White needles are intermetallic. The arrows indicate the direction of applied centrifugal force [18].

Functionally graded Aluminum- boron carbide composites have been produced by both centrifugal casting and type casting methods. The microstructure with varying processing parameters and the consequent graded hardness has been characterized [39].

Kumar et al. [40] studied functionally graded aluminum alloy in-situ composites (FG-AMCs) with TiB2 and TiC reinforcements synthesized by the horizontal centrifugal casting technique. Both Al-Si alloy (A356) and an Al-Cu alloy were used as matrices. The matrix and reinforcement type as well as process parameters like mold temperature, mold speed, and melt stirring were found to affect the gradient structure. Microstructural features with different processing parameters showed that the gradients in the reinforcement (Fig.2.8) modify the microstructure and hardness of alloy. The in-situ formed TiB_2 and TiC particulates modify the morphology of Si particles during the solidification. The stirring of the melt before pouring has the prominent effect on the segregating tendency of the reinforcements at different zones of the casting.

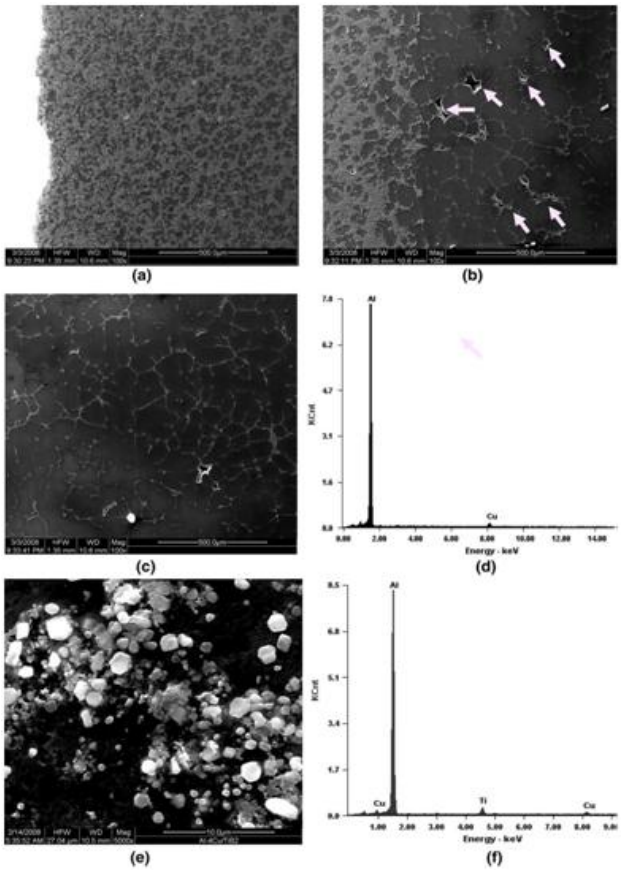

Fig.2.8. SEM micrographs of Al-4Cu-TiB_2 FG composite showing (a) outer, (b) middle, (c) inner region of the composite, (d) EDS spectrum from particle-free region, (e) high-magnification image from the outer region, and (f) EDS spectrum from one of the TiB_2 particles (speed of 2000 rpm with the mold temperature of 900°C)[40].

Al-AlB_2 FG composites fabricated by centrifugal casting have been studied by Z. Humberto Melgarejo et al. [41]. Both gravity casting and centrifugal castings were made from Al–5wt.%B and Al–4wt.%B–2wt.%Mg. The centrifugally cast materials caused the segregation of AlB_2 particles at the outer regions and consequently higher superficial hardness, microhardness and wear resistance towards the outer periphery of the casting are observed (Fig.2.9).

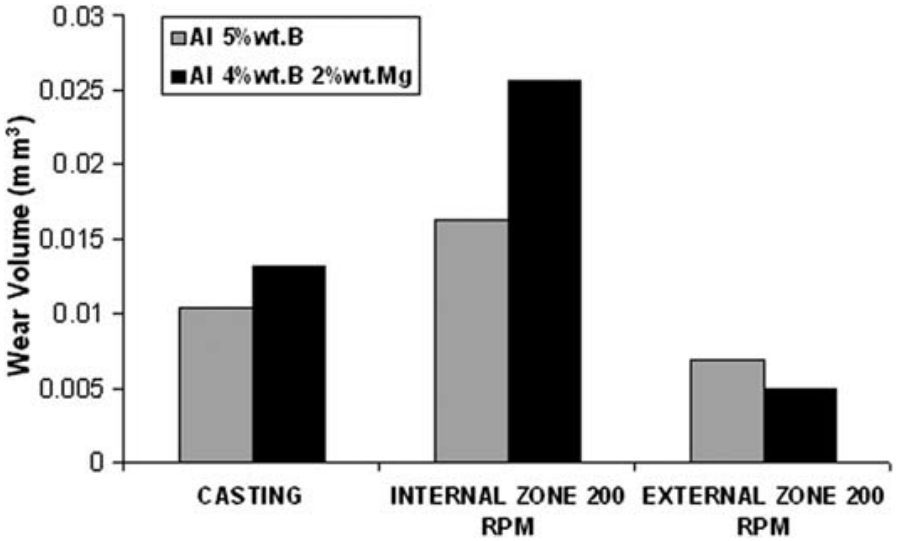

Fig.2.9. Wear volume for the various AMC samples subjected to pin-on-disk wear tests under identical conditions [41].

b) FGMs by application of magnetic and electromagnetic field

Magnetic and electromagnetic fields are widely employed in liquid metal processing. Several researches are reported on the effects of these two fields on particle movement in liquid slurry. Broadly, there are two types of magnetic field applications: 1) action on ferromagnetic particles in the production of reinforced ceramics by liquid processing routes, and 2) generation of Lorentz force in a liquid MMC leading to influence particle movement during solidification of the liquid matrix.

In-situ layered FGMs have beeniz synthesized by Changjiang Song et al.[42] by electromagnetic separation technique using the alloy of composition Al–22% Si–3.9% Ti–0.78% B. Three layers formed are 1) layer of primary ternary intermetallic compound Al–Si–Ti particles rich in Si; 2) the layer of the primary Si particles, and 3) layer of the Al–Si eutectic structure. The cause behind these layer formations under the electromagnetic field is due to difference in their temperature range of formation. The interfaces between two layers are gradually transitional in the microstructure (Fig.2.10). Due to the difference in

the electrical conductivity of the melt and primary particles, the electromagnetic Archimedes force will act on the primary particles and these will move in the direction of the electromagnetic Archimedes force.

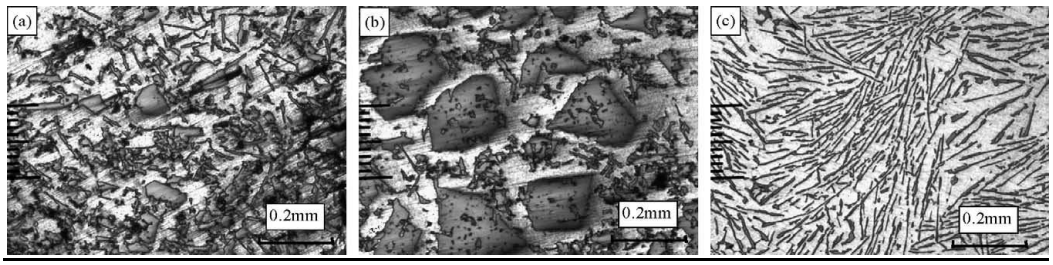

Fig.2.10. Microstructure of the in situ multi-layer FGMs by Electromagnetic Separation method: (a–c) are the microstructure of the first layer, second layer and the third layer respectively [42].

In another study by Changjiang Song et al.[43], the structure of in situ Al/Si FGMs under electromagnetic field has been found to change from Al–Si hypereutectic to eutectic and ultimately to hypoeutectic structure from one side of the sample to another. The volume fraction of Si particles and the resulting hardness are also showed gradient distributions (Fig.2.11).

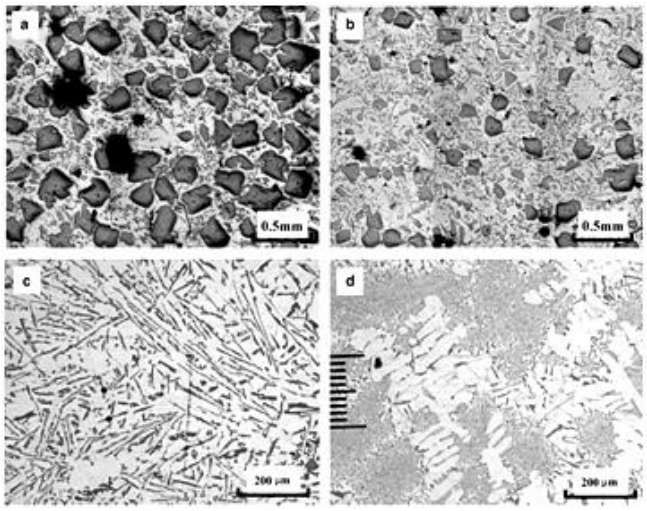

Fig.2.11. Microstructure of in-situ Al-Si FGM by electromagnetic separation method: (a), (b), (c) and (d) are microstructure of region from top of casting to bottom respectively [43].

The effect of processing parameters on Mg_2Si particle distribution in Al-Mg_2Si FGMs produced in-situ by electromagnetic field application [44]. The particle distribution is governed by Lorentz force, the solidification rate, and alloy composition. Higher Lorentz force results in decrease in the particle-rich region, and vice-versa. Al_3Ni phase distribution in in-situ Al-Al_3Ni FGMs under Lorentz force are also investigated [45]. Alloy compositions studied are Al-12 wt% Ni, Al-17 wt% Ni and Al-23 wt% Ni. The segregation pattern of the intermetallic Al_3Ni in the ingot is shown in Fig.2.12. In the region of enriched Al_3Ni the major axis of Al_3Ni particles aligns perpendicular to the Lorentz force. The size of Al_3Ni particles are refined in solidification under Lorentz force compared to that without this force.

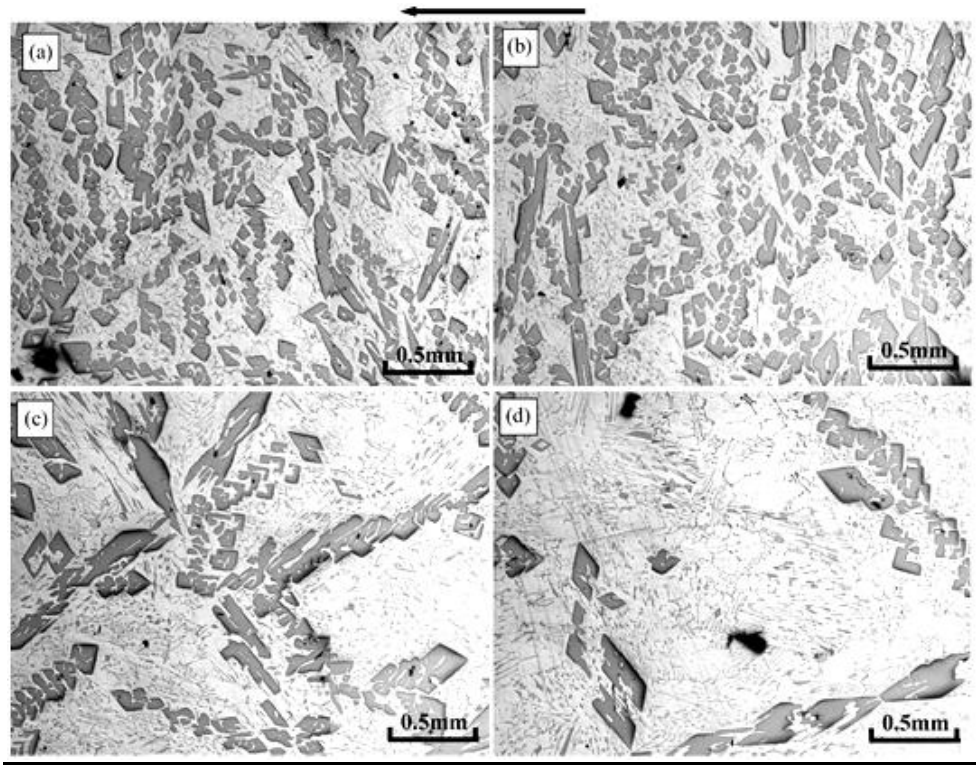

Fig.2.12. Microstructure of Al–17 wt.%Ni sample solidified under the electromagnetic field: (a), (b), (c), and (d) are microstructures of regions from bottom to top of casting respectively. Electromagnetic Archimedes force acts in the direction of arrow [45].

c) Infiltration processing

Infiltration processing is a suitable fabrication method for production of FGMs having phases with different melting points. In this process a refractory preform with a porosity gradient is produced and allowed to infiltrate at elevated temperatures with molten lower melting component [46]. It is necessary that, the preform contains open pores only and must be insoluble in the molten metal. The technique is specifically suitable for metal-ceramic and glass-ceramic FGMs. But metal-ceramic systems are usually non-wetting in nature (with a wetting angle $\Theta > 90^{\circ}$) and spontaneous infiltration through performs are difficult. Application of pressure during infiltration causes infiltration through larger pores. The required pressure p for a complete infiltration of a cylindrical pore of radius r_p is given by

$$p = -2\gamma_{LV} \cos\Theta / r_p$$

where γ_{LV} is the surface tension of the melt.

For a cylindrical pore in a ceramic/metal system with a pore radius of 5 μm, a wetting angle of 120^0 and a surface tension of 1 J/m^2 a pressure of 0.2MPa is necessary for infiltration.

Squeeze casting or gas-pressure sintering equipment are necessary for exerting pressures required for complete infiltration of real pore structures. Alternatively, the wettability is to be improved by pre-coating the preform, or changing the composition of the gas atmosphere. However, a high pressure iof 1atm is needed even for a wetting angle of about 30^0 for complete infiltration of a particulate preform [47].

Further, restricted availability of graded porous preforms without closed porosity and need for a sufficiently strong preform at high porosity to resist the applied pressure are other limitations of this process. Such preforms are reported [48] to be produced by graded sized

particle powder compacts. The particle size gradient leads to form porosity gradient on sintering [48]. Consolidation during sintering is required to avoid distortion. Other methods for production of graded preforms are sintering of green compacts with a graded content of short fibres [49], transformation of a Al-Al_2O_3 gradient into a porosity gradient during sintering [50], transformation of a gradient in carbon content in TiCx into a porosity gradient during sintering [51].

Al–4 wt.% Cu alloy reinforced with alumina fiber (Al_2O_{3f}) and alumina particulate (Al_2O_{3p}) (Hybrid-MMC) have been fabricated by a low pressure infiltration process [52]. Total amount of reinforcements is fixed to be 20 vol.% and the range of the amounts of Al_2O_{3f} and Al_2O_{3p} is varied from 7.5 vol.% to 12.5 vol.%. The castings were sound while the ratio of fiber vol.% to particle vol.% is increased. The Hybrid-MMC with 12.5 vol.% Al_2O_{3f} and 7.5 vol.% Al_2O_{3p} exhibits better wear resistance compared with particulate reinforcement with 20 vol.% Al_2O_{3p} and fiber reinforcement with 20 vol.% Al_2O_{3f}. The improvement in Hybrid-MMC can be attributed to a synergy effect of Al_2O_3 particles and Al_2O_3 fibers having a 3-D distribution, which protects Al_2O_3 particles from dropping out [53]. Further improvement in wear resistance has been observed in the MMC with an age-hardened Al–Cu matrix.

d) Directional solidification

The possibilities of generating a macroscopic, one dimensional concentration gradient with radial symmetry by directional solidification were also investigated [53]. The difference between the solidus and liquidus composition during directional solidification of an alloy is exploited for fabrication of FGM. To avoid steady state solidification under with constant solid concentration, the melt in front of the solidification front must be

stirred effectively. This condition can be achieved by natural convection in a vertical resistance furnace (Fig.2.13).

A temperature gradient was set by top cooling coils of the furnace. Samples were melted inside the furnace and allowed to proceed in the direction of the chilled zone with at fixed velocity. The solidification direction was thus in the upward direction, and for alloying elements with higher density than the matrix element, a solutally and thermally unstable density gradient in the melt was developed.

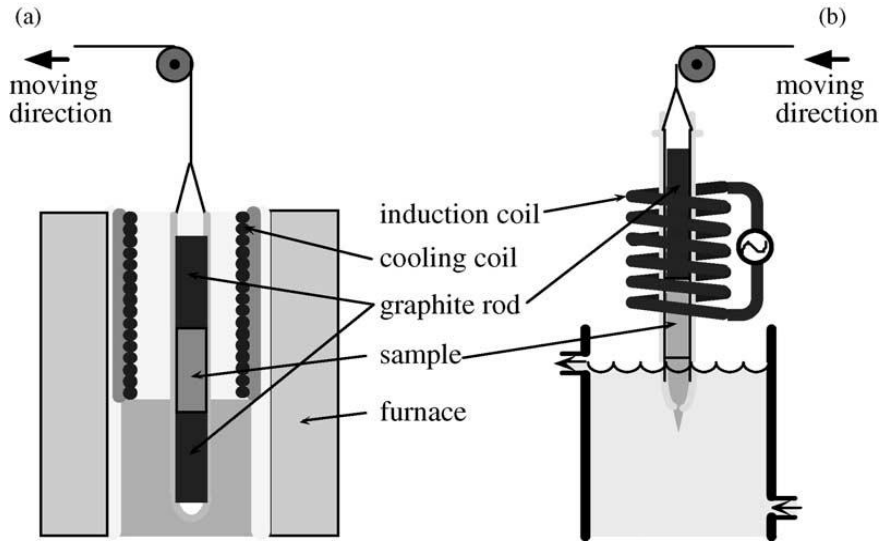

Fig.2.13. Set-up for directional solidification experiments a) with natural convection and b) with forced convection [53].

2.3. Al-Mg_2Si in-situ metal matrix composite

The Al-Si-Mg system has been established as a very promising system for the synthesis of Al matrix in situ composites, with the Mg_2Si intermetallic phase formed as reinforcing phase. Early researches on Al alloys have shown the advantages of Mg addition on the improvement of corrosion resistance and machinability. Moreover, the Si having high latent heat of fusion, enhances the castability. Si is a eutectic former with Al, thus

resulting sufficient fluidity for shrinkage compensation. The combined additions of Mg and Si at relatively high wt.% form of Mg_2Si intermetallic phase, emerging a new class of in-situ Al composite materials. This Al-Mg_2Si composites constitute a new category of superlight materials drawing significant interest for potential aerospace, automotive, and other hi-tech applications.The intermetallic compound Mg_2Si exhibits a high melting temperature of 1085°C, low density of 1.99× 103 kg m^{-3} , high hardness of 4500 MN m^{-2} , a low coefficient of thermal expansion (CTE) of 7.5×10^{-6} K^{-1} and a reasonably high elastic modulus of 120 GPa. Such a combination of properties makes Mg_2Si a potential reinforcement for Al-based MMCs. Similarities in properties and solidification behaviors between Mg_2Si and Si have been reported [54].

2.3.1. Morphology and growth mechanism of Mg_2Si in Al; effect of solidification rate

The morphology and the size of primary Mg_2Si particles have a large effect on the mechanical properties of materials. Hence, it is very much pertinent to understand the mechanism and control the growth of Mg_2Si. C. Li et al.[55] studied extensively the three-dimensional morphologies of primary Mg_2Si in Al–Mg_2Si alloys and its growth mechanism. Primary Mg_2Si crystals in the alloys are found to be in various geometric shapes, such as octahedron, hopper, truncated octahedron, cube and enormous dendrite (Fig.2.14). However, different shapes tend to form equilibrium shape of faceted octahedron to minimize the total surface free energy.

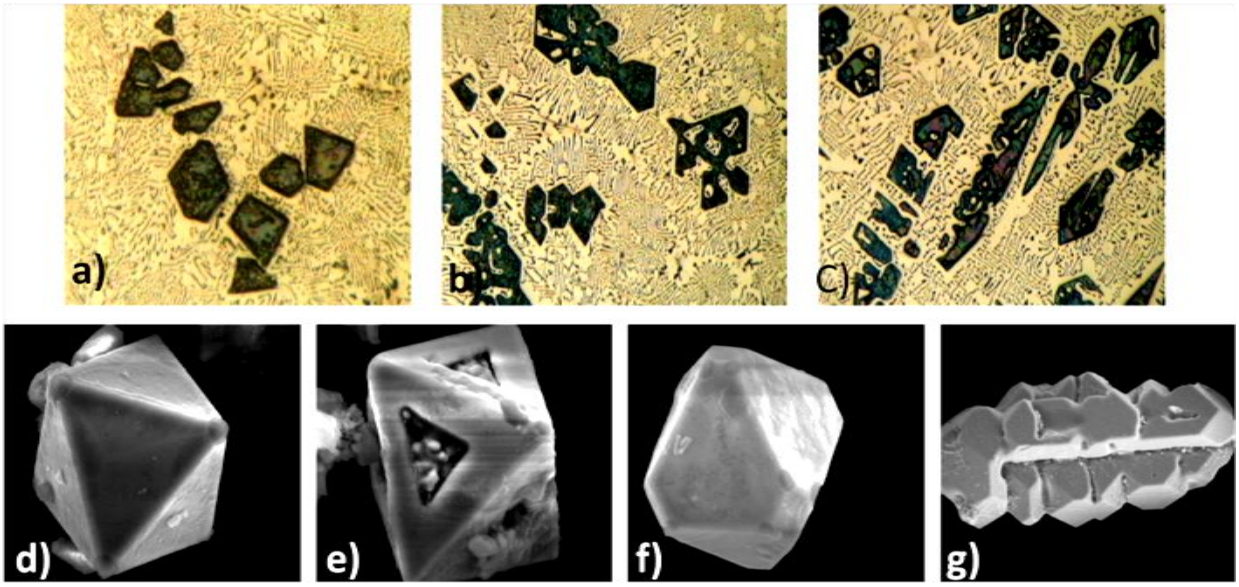

Fig.2.14. (a)–(c) Solidification microstructures of Al–x%Mg_2Si (x = 15, 20, 30) alloys: (a) x = 15; (b) x = 20; (c) x = 30. (d)–(g) Different three-dimensional shapes of the extracted primary Mg_2Si: (d) complete octahedron; (e) hopper; (f) truncated octahedron; (g) dendrite (Ref.55).

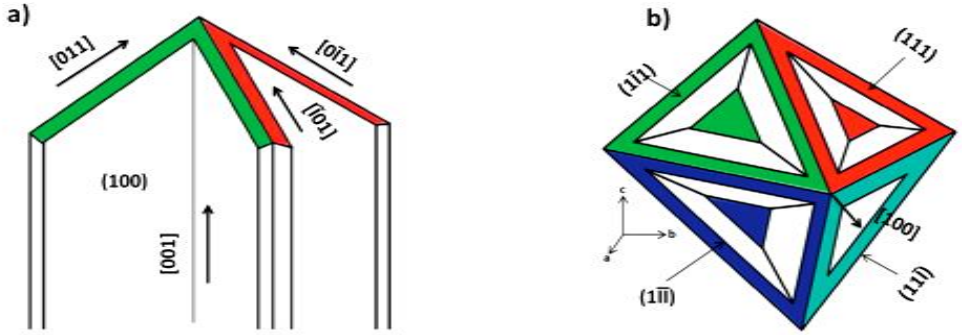

Fig.2.15. Schematic diagram showing growth of the octahedral profile: (a) directions of secondary branches at the advancing tip of the first branch in the [0 0 1] direction; (b) relationship between the corners and surfaces of the octahedral profile.(Ref.55)

Along <1 0 0> the higher growth rate results in the degradation of the six {1 0 0} facets to corners. But, because of their lower growth rates, eight {1 1 1} facets remain to form octahedron Mg_2Si. However, the growth velocities of the <1 0 0> and <1 1 1> directions can be controlled by means of external growth conditions, which are responsible for the evolution of Mg_2Si crystals into other morphologies (Fig.2.15).

Qin et al.[56] has investigated the effect of rate of solidification on the primary Mg_2Si particles' morphology. The rapid solidification causes a smooth surface cylindrical structure (Fig2.16). With decrease in solidification rate the morphology converts with slight angular features at free surfaces. Further lowering of solidification rate develops typical faceted morphology. They concluded that the mode of growth of high-melting entropy primary Mg_2Si in hypereutectic Al–Mg_2Si alloys changes from faceted to non-faceted type with increase in cooling rate and the critical transition solidification rate is about 10^6 ^{0}C/s.

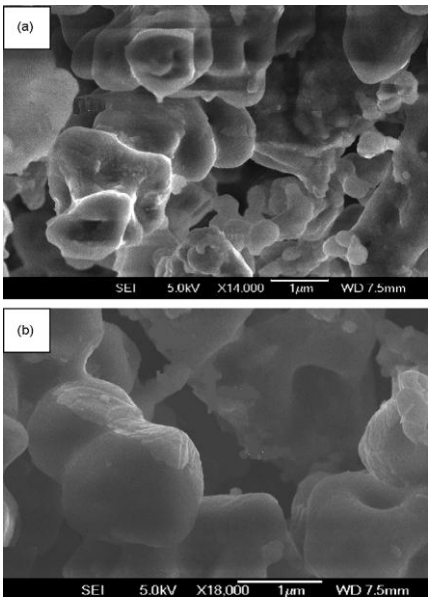

Fig.2.16. SEM image showing primary Mg_2Si in Al–Mg_2Si melt-spun ribbon: (a) slight angular features at free surface and (b) smooth surfaced cylindrical structure with rapid solidification.(Ref.56).

The change in morphology and number of primary Mg_2Si particles per unit volume in a hypereutectic Al-Mg-Si alloy with rate of solidification was studied by Zhang et al. [57] and Ourfali et al.[58].The longitudinal sections of wedge casting and Bridgman – solidified casting respectively were studied with different solidification rates. The longitudinal sections featured the three particulate morphologies of primary Mg_2Si

changing from irregular polyhedral to regular polyhedral and finally to dendritic as the cooling rates are faster.

2.3.2. Effect of different processing routes and solidification parameters on the microstructure and properties

a) Effect of intensive melt shearing

The effect of intensive melt shearing on the size, shape and distribution of primary phases and eutectics of a hypereutectic Al-Mg_2Si alloy has been studied by Hu-Tian Li et al [59]. Melt processing by advanced shear technology, a newly developed method for metal melt processing, subjects liquid alloys to high turbulence and intensive shearing. Intensive melt shearing disperses oxide films, intermetallic compounds, etc. and produces a uniform thermal fields and homogeneous composition. It also favors heterogeneous nucleation sites on these dispersed particles and grain refinement can be achieved. By intensive melt shearing of hypereutectic Al-Mg_2Si alloy, the coarse dendritic Mg_2Si are converted to refine compact polyhedral shaped Mg_2Si. Apart from the refinement of Mg_2Si, eutectic cell size and eutectic lamellar spacing in Al-Mg_2Si pseudo binary eutectic structures are also observed to be reduced. The refinement of microstructures of both primary Mg_2Si particles and eutectic cell size and lamellar spacing of (Al-Mg_2Si) pseudo binary eutectic was inferred due to heterogeneous nucleation on the dispersed oxide particles in the liquid Al-Mg-Si alloy by intensive shearing.

b) Effect of melt superheating treatment

The effect of superheating melt temperatures and holding times on the primary Mg_2Si particles in a commercial Al-20Mg_2Si-2Cu in situ composite were studied by Azmah Nordin et al.[60] and Qin et al.[61]. Melt superheating at around 950°C with a short holding time of 15 minutes was found to be the best parameter to cause appropriate

refining effect on the primary Mg_2Si particles (Fig.2.17). The corresponding microstructure shows refined polygonal shaped Mg_2Si. The cooling curve depicts an increase in the nucleation temperature, T_N, indicating the ease with which the particles nucleate and grow. With higher holding time causes coarsening of the Mg_2Si particles (Fig.2.4).

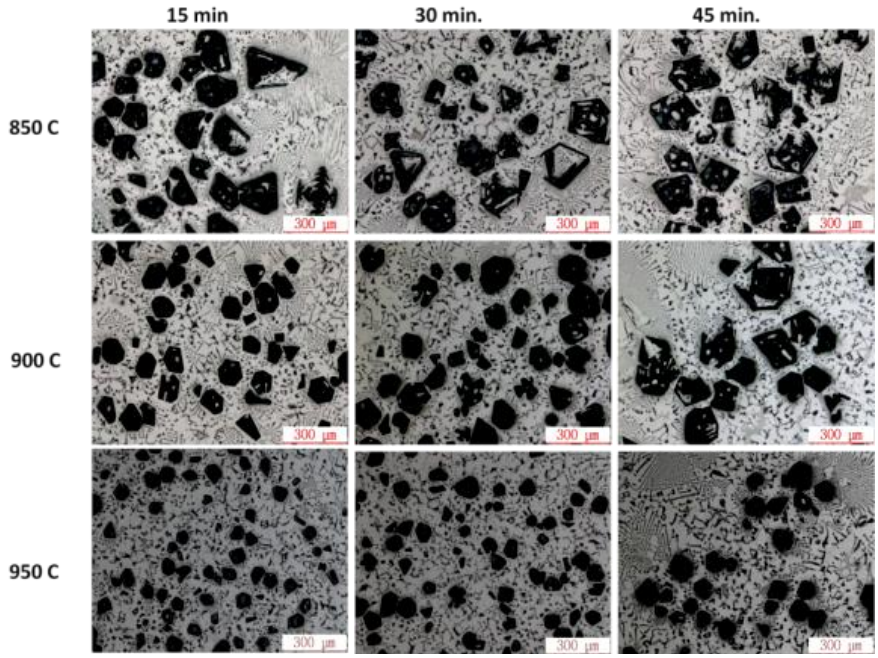

Fig.2.17. Modification and refinement of primary Mg_2Si particles at various superheat temperatures (850, 900, 950°C) and holding times (15, 30 and 45 minutes).(Ref.60).

c) Semi-solid processing

Among all the techniques of Semi-solid Processing, the cooling slope process is a simple route. The process involves pouring of molten metal with a suitable superheat through a cooling slope plate and subsequently allowed to solidify in a mold. As an effect the primary phase in the semisolid alloy has been reported to [62] become globular after remelting in the semisolid state. Qin et al. [62] fabricated an in situ Al–Si–Cu/ Mg_2Si composite with semisolid structure by cooling slope casting and partial remelting process.

They observed that, the morphology of primary Mg_2Si and α-Al grains in the composite are globular and/or elliptic after partial remelting process. The size and shape factor of α-Al grains increase with the isothermal holding time however the Mg_2Si particle size is unchanged with holding time (Fig.2.18).

The dendritic to spherical transition is inferred to be due to the liquid penetration through the as-cast grain boundary during the semisolid isothermal holding. This results in the fragmentation of the dendrite arms and subsequently to spheroidal or ellipsoidal grains.

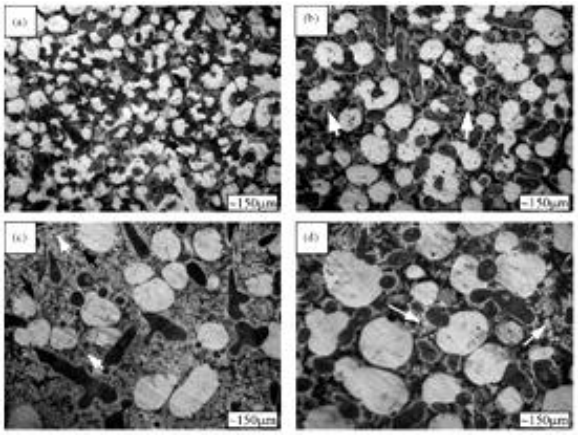

Fig.2.18. Semisolid microstructures of the Al- Mg_2Si composite by the cooling slope cast with different isothermal holding time of (a) 30 min, (b) 60 min, (c) 180 min and (d) 600 min.(Ref.62).

2.3.3. Effect of chemical modifications of Mg_2Si particles

a) Effect of extra silicon addition

Addition of extra Si to Al-Mg_2Si melt has a prominent effect on the refinement of morphology as observed by various researchers [63-66]. With increase in Si content up to 2 wt.%, the average size of primary Mg_2Si particles reduced and the volume fraction of α-Al phase increased. Further increase in Si content up to 7 wt.% causes increase in the average size of primary Mg_2Si particles with no significant change in the volume fraction of α-Al phase.

According to Fig.2.19 with the increase in Si content, the equilibrium solidification reactions of the alloys will change from (1) to (3) depending on the alloy compositions:

(1) Al-15Mg_2Si-(0-a)Si: $L \rightarrow L_1 + Mg_2Si_p \rightarrow L_2 + (Al+Mg_2Si)_E + Mg2Si_p \rightarrow (Al + Mg_2Si)_E + Mg_2Si_p$

(2) Al-15Mg_2Si-(a-b)Si: $L \rightarrow L_1 + Mg_2Si_p \rightarrow L_2 + (Al + Mg_2Si)_E + Mg_2Si_p \rightarrow (Al + Si + Mg_2Si)_E + (Si + Mg_2Si)_E + Mg_2Si_p$

(3) Al-15Mg_2Si-(b-c)Si: $L \rightarrow L_1 + Mg_2Si_p \rightarrow L_2 + (Si + Mg_2Si)_E + Mg_2Si_p \rightarrow (Al + Si + Mg_2Si)_E + (Si + Mg_2Si)_E + Mg_2Si_p$

where the subscript P indicates the primary particle, E indicates the eutectic, a, b and c indicate the composition range as marked in Fig.2.19.

The resulting microstructure reveals blocky Mg_2Si phase is enveloped by Al–Mg_2Si binary eutectic and then by Al–Mg_2Si–Si ternary eutectic structure. Primary Mg_2Si phase at the centres shows either dendritic or polyhedral morphologies. Al–Mg_2Si binary eutectic cells with regular morphologies have flake-like Mg_2Si surrounded by α-Al. Al–Mg_2Si–Si ternary eutectic cells distribute among binary eutectic cells and make binary eutectic cells separated to be relatively independent "islands"[66]. The tensile strength and ductility both were found to be improved up to 2% Si addition beyond that the effect is marginal (Fig.2.20).

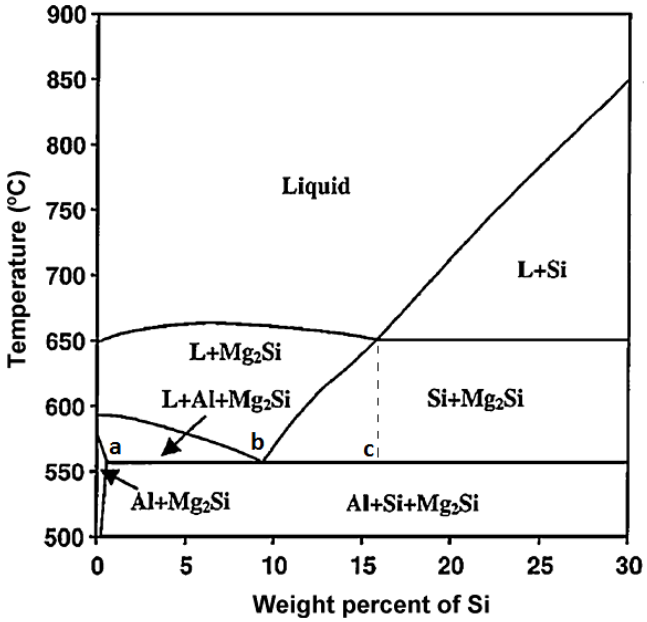

Fig.2.19. Calculated vertical section of Al–20%Mg_2Si to Si in the equilibrium Al–Mg–Si phase diagram (Ref. 63)

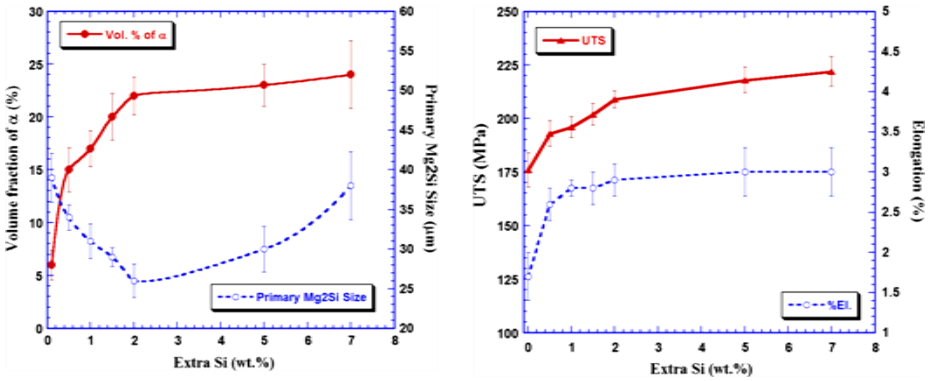

Fig.2.20. The primary Mg_2Si particle size and the volume percent of α-Al phase and the resulting properties as a function of extra Si content.(Ref.65).

b) Effect of extra Mg additions

The effects of Mg additions ranging from 6 to 15 wt.% on the solidification behavior of hypereutectic Al-15Si-4Cu-Mg alloy was investigated by Tebib et al.[67]. The Mg wt.% strongly influences the microstructural evolution of the primary Mg_2Si phase as well as the solidification behavior. The solidification paths in three range of Mg additions can be classified into three representative types (Fig.2.21):

Type I (Mg wt.% ranging from 5.16 to 12.5%):

$L \rightarrow L + Mg_2Si \rightarrow L + Si + Mg_2Si \rightarrow L + Si + \alpha\text{-}Al + Mg_2Si \rightarrow Q\text{-}Al_5Mg_8Cu_2Si_6 + Si + \alpha\text{-}Al + Mg_2Si$

Type II (Mg wt.% 12.5% eutectic composition):

$L \rightarrow L + Mg_2Si \rightarrow L + Si + \alpha\text{-}Al + Mg_2Si \rightarrow Q\text{-}Al_5Mg_8Cu_2Si_6 + Si + \alpha\text{-}Al + Mg_2Si$

Type III (Mg wt.% ranging from 12.5 to 15%):

$L \rightarrow L + Mg_2Si \rightarrow L + \alpha\text{-}Al + Mg_2Si \rightarrow L + Si + \alpha\text{-}Al + Mg_2Si \rightarrow Q\text{-}Al_5Mg_8Cu_2Si_6 + Si + \alpha\text{-}Al + Mg_2Si$

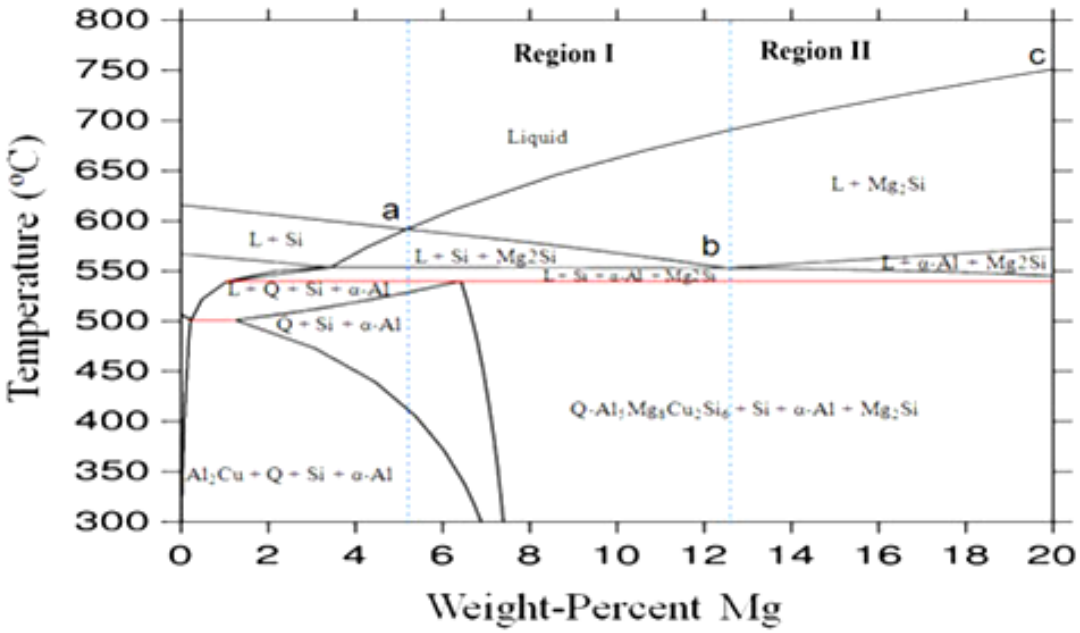

Fig.2.21. Calculated phase diagram of Al-Si-Cu-Mg system. The dashed lines represent respectively the critical compositions of Al-15Si-4Cu-xMg at 5.16 pct Mg and 12.52 pct Mg.(Ref.67).

The growth characteristics of the primary Mg_2Si is changing as observed by the evolution of Mg_2Si morphology with change in Mg contents. The morphology is changing from an octahedral to a faceted dendrite form(Fig.2.22).

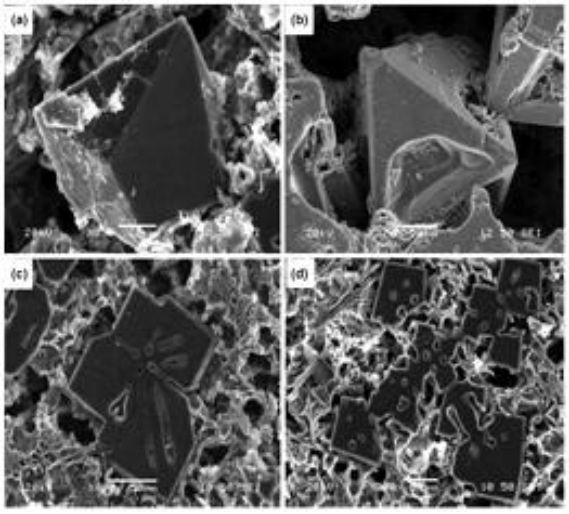

Fig.2.22. SEM micrographs showing the morphological evolution of Mg_2Si phase with increase in Mg wt.% addition: (a) 6.2%, (b) 8.4%, (c) 12.8% and (d) 14.9%.(Ref.67).

Feng Yan et al.[68] studied the effect of excess Mg addition in Al-Mg_2Si alloy high pressure die castings. Due to extra Mg addition, the eutectic point of the pseudo-binary Al-Mg_2Si system is lowered giving rise to an eutectic with lower Mg_2Si content. They observed the improvement in yield strength but reduction in tensile strengths and ductility after high pressure die casting. However, Al-8Mg_2Si-6Mg alloy offered an excellent combination of high strength and reasonable ductility.

c) Chemical modifications with different alloying elements and materials

Ghorbani et al. [69] studied the effect of Cr addition (0.5 wt.%–5 wt.%) on Al-15% Mg_2Si composites. They observed that, up to 2 wt.% Cr addition, not only refined the primary Mg_2Si particles, but also reduced interlayer distance of Mg_2Si phase in through eutectic cells. The hardness, strength and elongation values are reported to be improved. The improvement of the tensile properties is attributed mainly due to the reduction in potential sites for crack initiation and propagation path.

The high temperature tensile strength up to 350^0C has been observed to be increased by 23% by addition of Ni (~5%) to Al-20% Mg_2Si composites, as studied by

Chong Li et al. [70]. On addition of Ni, $NiAl_3$ phase forms in Al–Mg_2Si, and Al–Mg_2Si–$NiAl_3$ ternary eutectic structure appears with the increase of Ni content. At 5% Ni content, the Al–Mg_2Si binary eutectic is replaced by Al–Mg_2Si–$NiAl_3$ ternary eutectic, which is responsible for the improvement in high temperature (350^0C) tensile strength. Eutectic $NiAl_3$ phase tends to form rods with lower interfacial energy, compared with lamellar structure. This favors the formation of rod-like Mg_2Si rather than flake-like Mg_2Si. Finally, the unique double rod ternary eutectic structure is formed (Fig.2.23).

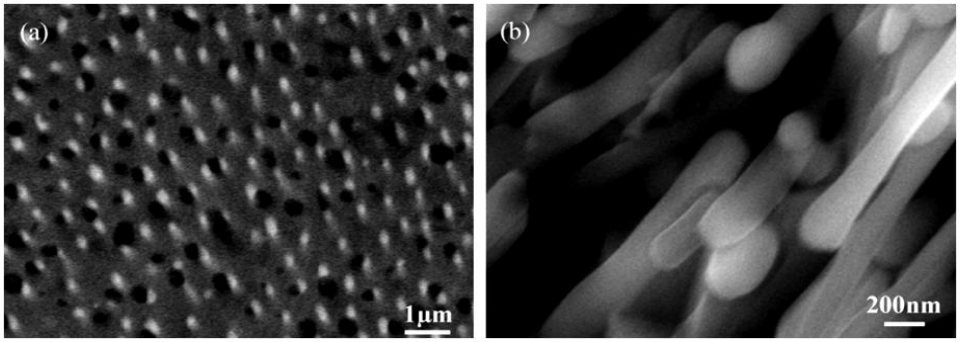

Fig.2.23. Microstructure of Al–$NiAl_3$–Mg_2Si ternary eutectic and (b) three-dimensional morphology after Al matrix is removed.(Ref.70).

Strontium addition to Al-Mg_2Si composites has very potent effect on refining of primary coarse Mg_2Si particles as reported by several researchers [71-74]. Size, density and aspect ratio measurements of Mg_2Si particles showed that addition of 0.01 wt.% Sr refined the Mg_2Si reinforcement. Beyond this percentage the Mg_2Si particles coarsens. From the thermal analysis it has been inferred that, Strontium addition caused a decrease in the nucleation and growth temperatures of Mg_2Si particles (Fig.2.24). The refining effect of Sr is likely to be related to the effect of oxide bi-films suspended in the composite melt as favored nucleation substrates for Mg_2Si particles.

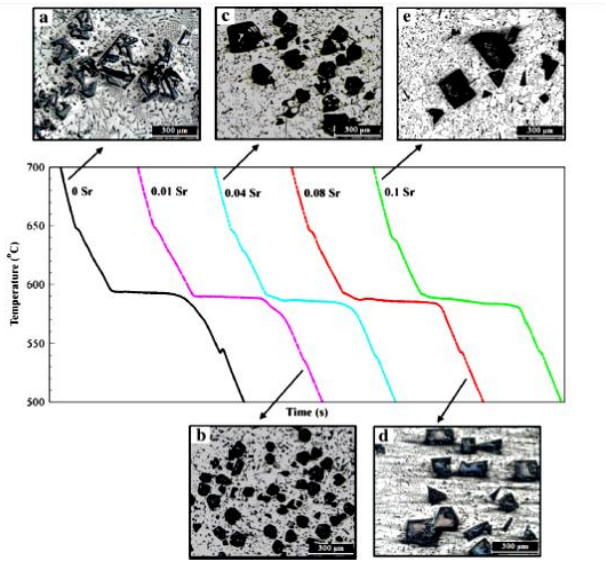

Fig.2.24. Cooling curves of composites and corresponding change in morphology at different concentrations of Sr: 0.01, 0.04, 0.08 and 0.1 wt.%.(Ref.73).

Farahany et al. [75] have investigated the effect of modification by Bi on Al-20%Mg_2Si-2%Cu alloy. An optimum modification effect was achieved with 0.4% Bi addition. Bi addition causes changes in morphology of primary and eutectic Mg_2Si. Consequent improvements in tensile strengths, hardness and impact toughness were resulted in by modification of both primary and pseudo-eutectic Mg_2Si crystals.

The effect of Lithium addition (ranging from 0.03-0.35 wt.%) on the microstructure and tensile properties of Al-15%Mg_2Si composites were studied by Hadian et al. [76-78] and Khorshidi et al.[79].

The additions have effects both on the morphology of primary Mg_2Si particles as well as eutectic Mg_2Si. The primary Mg_2Si changes from irregular or dendritic to polyhedral shape and size refines from 32 µm to 4 µm with 0.15 wt.% Li. The eutectic Mg_2Si phase alters from flake-like to coral-like. Further investigations on tensile tests revealed optimum Li level (0.15%) for improving both UTS and elongation values.

The effects of different types of rare earth elements and mischmetal addition on microstructural evolution of Al-Mg_2Si composites and the resulting mechanical properties have been investigated by several researchers [80-87]. The cerium addition up to 0.4 wt.% shows a refinement of primary Mg_2Si and its shape is polygonal and equiaxed [80]. However, with further increase in cerium content up to 1% the size of the Mg_2Si increases (Fig.2.25). The possible explanation for refinement of primary Mg_2Si is due to increase in number of nuclei leading to the changes of the morphology and size of primary Mg_2Si particle. Also, Ce addition suppresses the growth of primary Mg_2Si by modification of both the solid-liquid interfacial energy and the surface energy of the solid Mg_2Si phase. The morphology of the eutectic phases are also changed; without Ce addition, the eutectic Mg_2Si and eutectic Si are identified as flake-like morphology. With Ce addition eutectic Si changes from flake-like to coral-like morphology, and eutectic Mg_2Si changes to chrysanthemum-like (Fig.2.26). In another study by Nordin et al.[81], the modification effect of Ce in Al-20%Mg_2Si was observed up to 0.8 wt.% Ce, exceeding this percentage has no significant effect. Apart from change in primary Mg_2Si to polygonal shape Ce addition caused a better uniform distribution of the particles. The flake like eutectic Mg_2Si was changed to rod-like shape. These refining effects can be attributed to restricted growth theory by which the primary and eutectic Mg_2Si growth have been restricted by the formation of $Al_2Si_{12}Ce$ and $Al_7Si_{3.5}Ce$ intermetallcs.

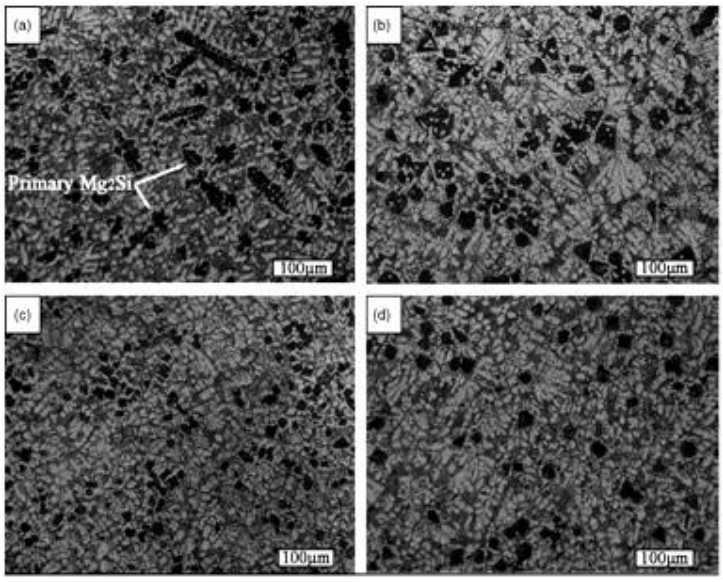

Fig.2.25. Optical microscope microstructures of in situ Mg_2Si/Al–Si–Cu composites with different Ce addition: (a) 0 wt.%; (b) 0.2 wt.%; (c) 0.4 wt.%; and (d) 1.0 wt.%.(Ref.80).

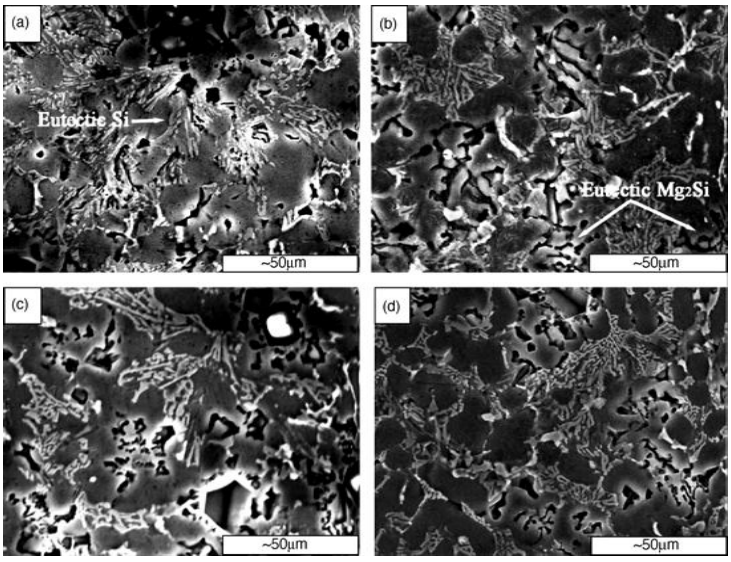

Fig.2.26. SEM images of the eutectic matrix in the composites with different Ce addition: (a) 0 wt.%;(b) 0.2 wt.%; (c) 0.4 wt.%; and (d) 1.0 wt.%.(Ref.80).

The modifying effect of yittrium addition on the primary and eutectic Mg_2Si in as-cast and heat treated conditions of Al alloy matrix [82,83] and Mg matrix [84] has been studied. It is observed that, the size and morphology of primary Mg_2Si are not changed considerably however; Y addition causes the pseudo-eutectic Mg_2Si to be changed from a flake-like to fine fibrous or rod-like morphology (Fig.2.27). An optimum Y additions can

reduce the amount of Mg_2Si phase dissolving into the matrix, promotes the precipitation of Al_2Y phase improving the mechanical properties. A linear increase in tensile strength up to an addition of 1% Y was observed in solution treated condition at 520°C for 4 h (Fig.2.28). The maximum UTS and elongation at room temperature for the heat-treated composites are 294 MPa and 7.4%, respectively.

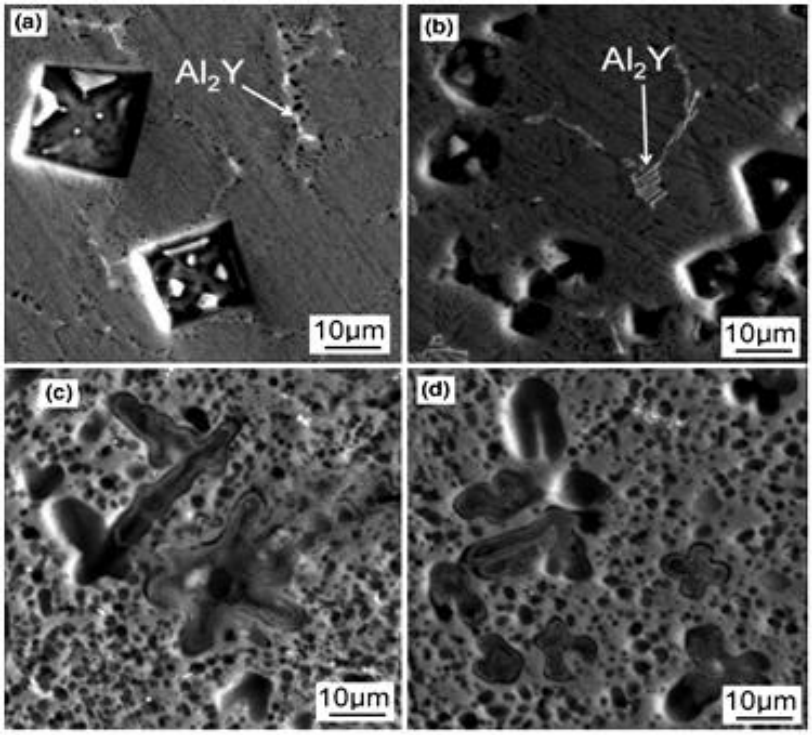

Fig.2.27. SEM micrograph of as-cast Al-15% Mg_2Si composite containing (a) 0.5 wt.% Y, (b) 1 wt.% Y , (c) and (d) are solution-treated composites containing 0.5 wt.% Y and 1 wt.% Y respectively.(Ref.83).

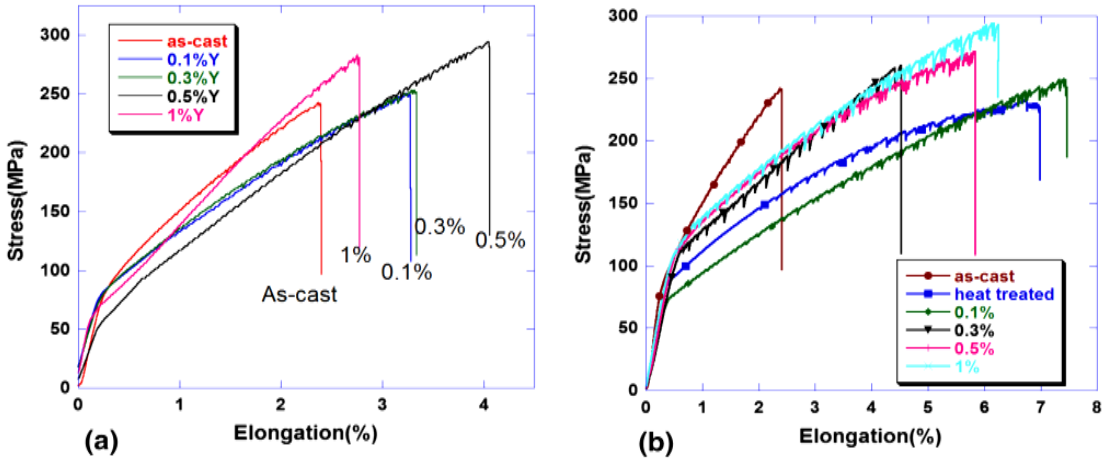

Fig.2.28. Engineering stress vs. elongation of Al-15% Mg_2Si composites containing various amounts of Y (a) before and (b) after solution treatment (Ref.83).

The modifying effect of Nd on the primary and eutectic morphology of Mg_2Si in Al-18 wt.% Mg_2Si has been investigated by Xiao Feng et al. [85]. The primary Mg_2Si morphology is changed from dendritic to polyhedral shape with refinement and the eutectic Mg_2Si is changed from flaky to coral-like or short fibrous. The refinement of Mg_2Si crystals by the addition of Nd is perhaps due to constitutional supercooling by the segregation of Nd in front of the solid/liquid interface of Mg_2Si during solidification.

AlNd phase has been detected with addition of 0.8 wt.% and above Nd. The dry sliding wear characteristics of these Nd treated alloy shows decreased wear rates and frictional co-efficient. The addition of 0.5 wt.% Nd results in a change in wear mechanism from combined abrasive, adhesive and delamination type wear to simply mild abrasive wear.

Similar to Nd, the modifying effect of La-intermetallic has been observed on Al-15 wt.% Mg_2Si[86]. The $LaSi_2$ phase has been detected to form during solidification due to La. With the addition of 0.3% La, UTS is decreased from 217 to 199 MPa and elongation values decreased from 5.5 to 4.2 %, but after adding 3%La, UTS is increased to 223 MPa and elongation values increased to 6 %.

Zhang et al. have studied the effect of mischmetal, a mixture rare earth elements, addition on Al- 15 wt.% Mg composite [87]. The addition causes a considerable reduction in the size of primary Mg_2Si particles and the pseudo-eutectic Mg_2Si was changed from a fibrous to a flake-like morphology, showing a divorced character. The rare earth elements present in mischmetal form $Al_{11}RE_3$ type of compounds which appeared to have strong influence on the nucleation process of primary Mg_2Si as well as the formation of α-Al and the pseudo-eutectic matrix. The volume% of α-Al increases steeply up to 0.8 wt.% mischmetal and then it becomes steady with further additions. In another research Zheng et al. [88], studied the effect of addition of rare earth oxides and $CaCO_3$ either singly or in combination. The combination showed the best modifying effect on the primary Mg_2Si and the matrix. They inferred the effect is due to 1) enrichment of rare earth compounds at the solid-liquid interface results in constitutional supercooling and 2) in a binary Ca-Si, $CaSi_2$ compound is formed and this is acting as nucleating sites for Mg_2Si to grow, improving morphology and refinement of the same.

Ghandvar et al.[89] have recently reported the effect of Gadolinium (Gd) addition for modification of Al-15%Mg_2Si in-situ composites. Addition of 1.0 wt.% Gd, modified the primary Mg_2Si morphology from coarse dendritic to fine octahedral shape. Change in morphology is associated with refinement and increased population density of Mg_2Si particles. The mechanism of modification has been proposed due to formation of very fine Al_3Gd particles generating sites for heterogeneous nucleation for Mg_2Si. Another possibility of modification is due to the poisoning by adsorption of Gd atoms preferentially on {100} facets of Mg_2Si crystals.

Phosphorus is reported to have a very prominent modifying effect on primary and eutectic Mg_2Si morphologies [90,91]. The effect is perhaps due to the effect of heterogeneous nucleation. As the volume is not changing increasing number of particles implies number of Mg_2Si nuclei. During the growth stage Mg_2Si crystal, without P addition, coarse dendrites are formed via formation of octahedron, while with P addition it is ultimately grow to tetrakaidecahedron (Fig.2.29). Holding temperature and time of the melt are the controlling factors affecting the modification.

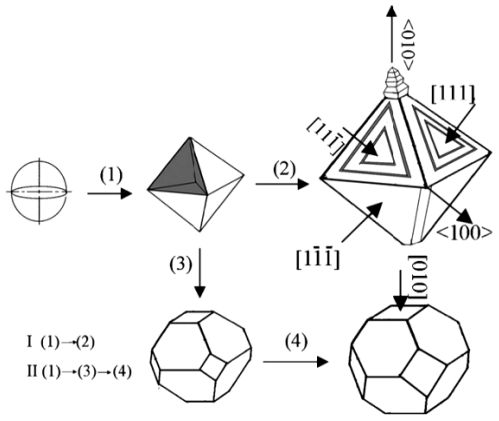

Fig.2.29. Stages of primary Mg_2Si crystal growth; without P addition (route 1 to 2), and with P addition (route 1 to 3 to 4) (Ref.90)

The refining effect on the primary Mg_2Si particles are reported by additions of salt mixture (A mixture of NaCl, NaF and KCl at a ratio of 15 : 35 : 10 wt %) [92] and addition of K_2TiF_6 [93]in the Al-Si-Mg melts. The refining effect mechanism is not yet clear; it might be due to either by poisoning the surface of Mg_2Si nuclei through the segregation of sodium in case of salt mixture or potassium in K_2TiF_6 at the liquid–solid interface or by changing the surface energy of Mg_2Si crystals by lattice distortion due to the existence of sodium/potassium in Mg_2Si lattice.

2.4. Functionally graded in-situ Al-Mg_2Si composites

Functionally graded (FG) materials are a new class of structural materials comprising of varied gradient composition and microstructure from one end to the other end. Among the various routes of fabrication of functionally graded metal matrix composites, centrifugal casting technique is most potential technique. The centrifugal force is applied in the liquid melt containing in-situ solid reinforcement particles and these are segregated either along the outer or inner surface of the casting due to the difference in density between the matrix and reinforcement. Various in-situ formed reinforcements in aluminum matrix FG-composites have been studied and Al-Mg_2Si composite is a highly potential FG composite. In hypereutectic Al-Si matrix FG composites the reinforcing particles are primary Si and Mg_2Si having densities ρ_{Si} = 2.33 g/cc and ρ_{Mg2Si} = 1.99 g/cc; both are smaller than that of Al melt (ρ_{Al} =2.37 g/cc). Consequently, reinforcements are segregated in the inner layer of the casting under the action of centrifugal force. Several researches have been made based on the development of Al-Mg_2Si FG composites [94-105].

Jian Zhang et al. reported [94, 95] the fabrication of Al-Mg_2Si FG composites by centrifugal casting. The Mg_2Si particle segregation causes increase in the hardness and tensile strength but decrease in elongation%. The particle distribution with different rotational speed and rate of cooling during solidification were assessed [95]. Lower rotation speed resulted in better gradient distribution of Mg_2Si primary particles but with increased casting defects. With the increased rotational speed, the thickness of the outer periphery containing particles is increased. A more refined microstructure in the outer

periphery is observed with the high cooling rate in a water cooled copper mould compared to that in graphite mould.

XIE Yong et al. [96] investigated the various parameters viz. rotational speed, mold pre-heating temperature and pouring temperature, affecting the distribution of primary Si and Mg_2Si particles in FG hypereutectic Al-19Si-5Mg alloy-Mg_2Si composite (Figs.2.30 and 2.31). When the centrifugal speed was increased, the volume fraction of Mg_2Si and primary silicon are increased in the inner layer, and decreased in the middle layer and outer layer. The population of these particles in the inner layer is increased when the pre-heating temperature of the mold is increased. This can be attributed to a longer solidification period of the molten metal in the mold. A higher pouring temperature leads to higher volume% of the particles in the inner layer because of longer solidification period of molten metal.

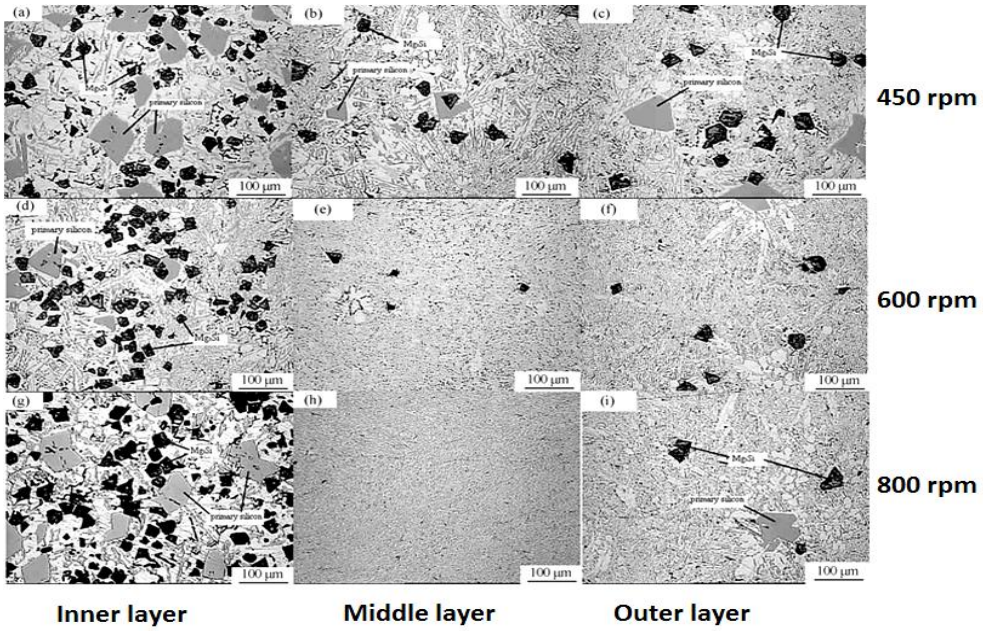

Fig.2.30. Variation of segregation tendency of primary Si and Mg_2Si particles at different layers of FG composites with different speed of rotations.(Ref.96).

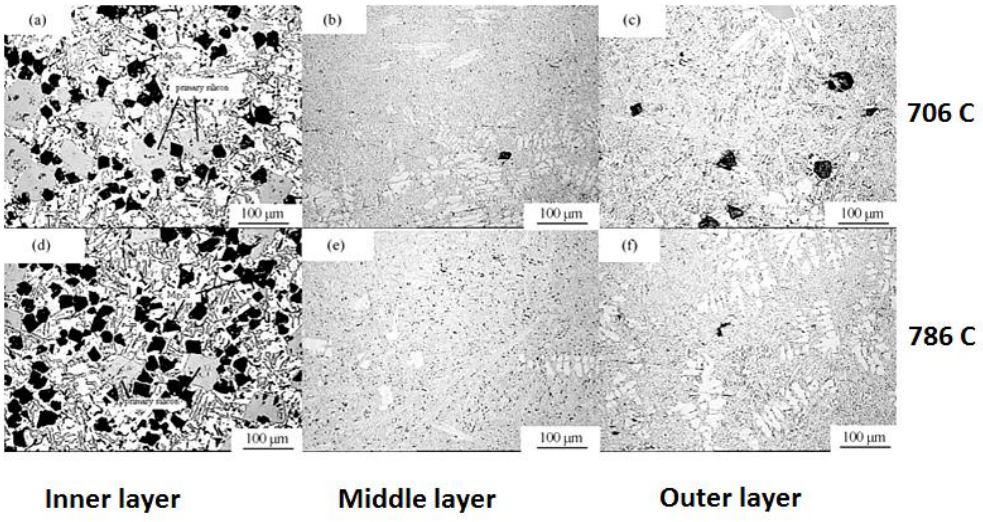

Fig.2.31. Variation of segregation tendency of primary Si and Mg_2Si particles at different layers of FG composites with different pouring temperatures as indicated.(Ref.96).

ZHAI Yan-bo et al. [97,98] investigated the graded distribution of primary Si particles in FG Al-19%Si alloy and Si and Mg_2Si particles in FG Al-19Si-5Mg alloy. The primary Si particles are small and almost evenly distributed throughout the cross-section however in Al-19Si-5Mg both primary Si and Mg_2Si are wrapped up and adhere together and segregated in the inner layer of the casting (Fig.2.32). The tubes of Al-19Si-5Mg possess a higher hardness and wear resistance than the tube of Al-19Si in the inner layer.

Fig.2.32. Mechanism of primary Si wrapping of Mg_2Si particles and adherence in the inner layer (Ref.97)

HAO Xuhong et al.[99] has investigated the development of automobile pistons made of hypereutectic Al-20Si-4Mg alloy FG composites by vertical centrifugal casting method. In situ primary Si and primary Mg_2Si particles were segregated at the regions of piston top and piston ring grooves. As a result the hardness and wear resistance are considerably enhanced which are further improved by solution treatment and ageing.

Xuedong Lin et al.[100] investigated the influences of various process parameters on the particle segregation ratio and the particle distributions of in situ primary Si/Mg_2Si particles in tubes of Al–Si–Mg functionally graded materials. The FG composites are intended for use in automobile liners. The process parameters studied were pouring temperatures, mold temperatures and G numbers ($G = \omega^2 R/g$, where R is the radius of the cast tube in m, ω is the mold rotation rate in radians s^{-1} and g is the acceleration due to gravity). The influences of these parameters on the particle segregation ratio, k, and the particle distributions involving the particle size and volume fraction were assessed. The particle segregation ratio was defined as $k = \alpha/L$, where α is the width of the reinforcement layer, and L is the thickness of the whole cross section from the inner wall to the outer wall along the radial direction. With the pouring temperature 720°C and mold temperature 90°C, and G > 60, particles are substantially segregated in the inner layer. But, when G < 40, the reinforcement layer could not be formed, and the particles distributed throughout the whole cross section. With high pouring or mold temperatures or large G numbers, the particle size of primary Si and Mg_2Si showed a graded distribution in the reinforcement.

Bo LI et al.[101] have evaluated the elevated temperature tensile properties of Al-20Si-5Mg alloy FG composite of reinforced as well as un-reinforced zones. A maximum ultimate tensile strength was observed at 100 °C for a good fitness in strength between matrix and reinforcements. The fracture surfaces showed macroscopically brittle fracture.

The mechanism of failure at lower temperature is due to particle fracture while particle/matrix decohesion is responsible for higher temperature failures.

Rahvard et al. [102] have studied the effect of addition of Mg to A390 alloy FG composite and their wear properties. With base alloy A390 without any Mg addition, primary Si is the reinforcement and was found to be distributed both in inner and outer layers. This is because the density of primary Si is a little lower than that of the base alloy. In case of 6% Mg addition both primary Si and Mg_2Si are segregated at inner layer only. As a result, the best wear resistance and hardness belong to the inner layer. When the Mg% was increased to 12%, the primary Mg_2Si as a reinforced particle is distributed near the entire cross-section, but only the narrow free reinforcement area in the middle layer. High Mg content is the main reason for producing this distribution characterization. The best wear resistance and hardness belong to the outer layer as well.

2.4.1. Effect of solution treatment and ageing

The effect of solution treatment and ageing on monolithic Al-Si, Al-Si-Cu, Al-Si-Mg and Al-Si-Mg-Cu alloys as well as Al-Mg_2Si in-situ composites has been well studied by various researchers. A large number of papers are based on characterization of the ageing sequence and precipitate morphology [103-110].

Qin et al. [111] studied the effect of solution treatment and ageing on Al-25Mg_2Si-3Si-3Cu-0.5P composite. The low melting phases dissolve into the matrix more easily and transforms to fine intermetallics [58]. The peak-aged unmodified composite had a UTS of 190 MPa with an elongation of 1.08%, while the UTS of the modified composite was 249 MPa with an elongation of 1.35%. The tensile strength and elongation of modified composites increase 31.1% and 25%, respectively. Similar effect was observed by Malekan

et al.[112] and Nasiri et al.[113]. They have investigated effect of solution treatment at different temperature on the morphology of primary and eutectic Mg_2Si phase. With increase in treatment temperature although sizes of primary Mg_2Si are not significantly changed, the sharp edges are rounded –up as the diffusion takes place predominantly from these locations in to the matrix. So far as the effect on matrix Mg_2Si morphology is concerned these are changed to fine dot-like and the eutectic network is partially broken (Fig.2.33).

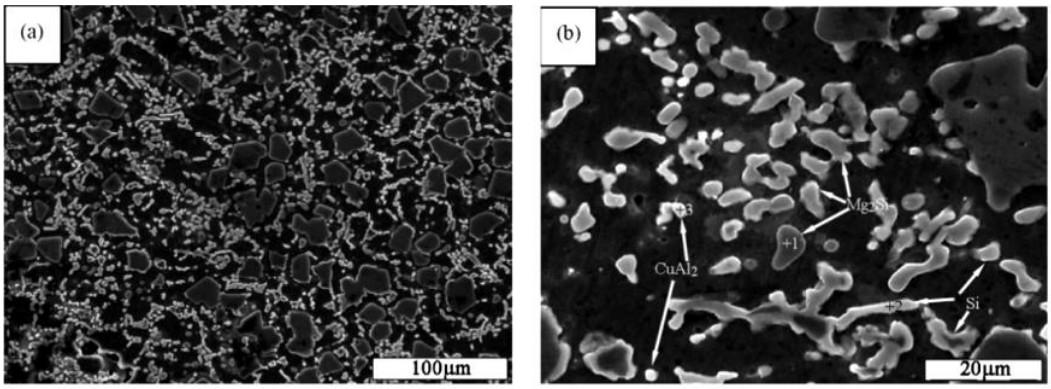

Fig.2.33. Effect of ageing treatment of Mg_2Si/Al composite after modification with phosphorus (a)low magnification and (b) high magnification (Ref.111).

Zedi Li et al. [105] studied the effect of heat treatment on microstructure and mechanical property of Al-10% Mg_2Si composite. When this composite was subjected to solution treatment at 520°C for 6 h and subsequent aging at 200°C for 6 h, long rod-like eutectic Mg_2Si were converted to short fiber-like and spherical morphologies. This is due to the fragmentation and spheroidization of eutectic Mg_2Si. Apart from this a large number of nano-sized particles were formed. The combined effect of these two depicts a significant improvement in ultimate tensile strength (234.6 MPa, 26% higher than that of cast alloy).

Chong Li et al. [114] investigated the effect on microstructural features and corrosion behavior of Al-10%Mg_2Si composites by heat treatment. They attributed the

change in eutectic Mg_2Si morphology is due to the existence of concaves and convexities on the long branches of Mg_2Si along the interface between Mg_2Si phase and Al matrix. During solution treatment and ageing, Mg and Si atoms diffuse continuously from the position with large curvature. The spheroidization takes place due to breaking of concaves of long Mg_2Si branches into sub-particles. Dissolution due to diffusion from eutectic Mg_2Si phase continues to reduce the surface energy. The transformation of eutectic Mg_2Si phase suppresses the rapid expansion of corrosion pits, which leads to enhancing the corrosion resistance of Al–10%Mg_2Si alloy.